UCRL-11102

University of California

Ernest O. Lawrence Radiation Laboratory

TWO-WEEK LOAN COPY

This is a Library Circulating Copy which may be borrowed for two weeks. For a personal retention copy, call Tech. Info. Division, Ext. 5545

DIFFUSION INDUCED DISLOCATIONS IN SILICON

Berkeley, California

DISCLAIMER

This document was prepared as an account of work sponsored by the United States Government. While this document is believed to contain correct information, neither the United States Government nor any agency thereof, nor the Regents of the University of California, nor any of their employees, makes any warranty, express or implied, or assumes any legal responsibility for the accuracy, completeness, or usefulness of any information, apparatus, product, or process disclosed, or represents that its use would not infringe privately owned rights. Reference herein to any specific commercial product, process, or service by its trade name, trademark, manufacturer, or otherwise, does not necessarily constitute or imply its endorsement, recommendation, or favoring by the United States Government or any agency thereof, or the Regents of the University of California. The views and opinions of authors expressed herein do not necessarily state or reflect those of the United States Government or any agency thereof or the Regents of the University of California.

Submitted for publication in Journal Applied Physics UCRL-11102

UNIVERSITY OF CALIFORNIA

Lawrence Radiation Laboratory
Berkeley, California

AEC Contract No. W-7405-eng-48

DIFFUSION INDUCED DISLOCATIONS IN SILICON

J. Washburn, G. Thomas, and H. J. Queisser

January 1964

DIFFUSION INDUCED DISLOCATIONS IN SILICON

J. Washburn and G. Thomas

Inorganic Materials Research Division, Lawrence Radiation Laboratory
and Department of Mineral Technology, University of California
Berkeley, California

H. J. Queisser

Clevite Semiconductor Division, Palo Alto, California
Present address: Physikalisches Institut, Universität Frankfurt, Germany

January 1964

Abstract

Plastic deformation produced by phosphorus diffusion into an (001) silicon surface has been studied by transmission electron microscopy. The lattice parameter differences in regions of steep solute concentration gradient are accommodated by a crossed grid of edge dislocations having Burgers vector a/2[110] and a/2[$\bar{1}$10]. The long edge dislocations end at nodes which suggests that they are formed by dislocation reactions between pairs of dislocations that can glide into the crystal on {111} planes.

Introduction

Lattice parameter variations accompanying gradients in concentration of a solute cause internal stresses in a crystal. If these stresses exceed the yield stress, plastic relaxation introduces an array of dislocations into the region of sharpest gradient.

In silicon, diffusion treatments (with boron, phosphorus or other doping elements), are frequently employed to achieve desirable electrical characteristics. Etch patterns at the surfaces through which the solutes are introduced show that local plastic deformation somtimes occurs.(1) The resulting dislocation array in boron or phosphorus diffused silicon has also been observed through etch pits on planes perpendicular to the diffusion front(2) and by x-ray diffraction contrast.(3)

The present experiments were undertaken to further study the character of diffusion induced plastic deformation and the resulting networks of dislocations in order to clarify the mechanism by which they move into the crystal as the diffusion proceeds.

Experimental

Slices were cut in the [001] orientation from crucible-grown silicon single crystals. The slices were lapped, mechanically polished, chemically etched and cleaned. A phosphorus "prediffusion" was then performed in the following manner: The slices were placed in the hot zone (1000 to 1300 °C) of a two-zone furnace. The cold zone (250°C) housed a supply of phosphorus pentoxide, which served as a source for n-type doping. A nitrogen stream carried the dopant into the hot zone. Silicon treated in such a way attains a surface film, generally assumed to consist of a glassy mixture of silicon and phosphorus oxides. Diffusion of phosphorus from this surface layer into the bulk causes formation of n-type layers.

The slices thus treated were prepared for transmission electron microscopy as described previously.[4] Observations were made in a Siemens Electron Microscope operated at 100 Kv and fitted with a special specimen stage that allowed tilting of the normal to the specimen surface to ±6° in any direction away from the axis of the microscope.[5] The analyses described in the paper could not have been done with only a simple tilting stage, (e.g., the standard stereo mechanism), because it was necessary to achieve a variety of single diffraction conditions for the same field of view.

Results and Discussion

Description of the dislocation geometry and the diffraction conditions will be facilitated by reference to the tetrahedron of {111} planes shown in the (001) projection in Fig. 1. The edges of the tetrahedron represent the six <110> directions and also the Burgers vectors of the type a/2<110>. Their projections onto (001) designated as (1), (2), (3), (4) will also be used to identify the traces of the diffraction planes that correspond to 400, 040, 220, and $\bar{2}20$ beams respectively. The criterion for visibility of the dislocations is that $\vec{b}$ must not lie in the reflecting plane (i.e., $\vec{g}\cdot\vec{b} \neq 0$).[6,7] Table I shows the dislocations that are visible for different reflections obtained in [001] films.

As shown at low magnification in Fig. 2a the dislocation network is a crossed grid of very long dislocation lines. They are somewhat wavy but on the average lie along the directions AD and BC (Fig. 1). To best accomodate an increase in lattice parameter on going from the surface to the interior they should be edge dislocations with Burgers vectors BC and AD respectively. The diffraction contrast results presented in Fig. 2(b,c,d) are consistent with this hypothesis (Table I). All the lines are present for diffraction plane (1) which does not contain either AD or BC. However, the lines parallel to AD, which should have BC as Burgers vector, go out of contrast for diffraction

Table I.

Visibility Criteria for Dislocations (Foils in [001])

$\vec{b}$ \ reflection	$\vec{g}\cdot\vec{b}$ (1) 400	(2) 040	(3) 220	(4) $\bar{2}20$
a/2[01$\bar{1}$]	0	2	1	1
a/2[$\bar{1}$0$\bar{1}$]	-2	0	-1	1
a/0[011]	0	2	1	1
a/2[$\bar{1}$01]	-2	0	-1	1
a/2[$\bar{1}$10]	-2	2	0	2
a/2[110]	2	2	2	0

The numbered planes refer to those shown in Fig. 1.

plane (4) as expected. The lines lying along BC that should have AD as Burgers vector are invisible when the diffraction plane is (3).*

It can also be shown that the parallel dislocations in each set of the networks are all of the same sign. If the foil is oriented for two diffracting beams, making an obtuse angle, double images are formed. In Fig. 3 the $\bar{4}00$ and 220 reflections operated. Notice the weaker secondary image is always to the same side as the strong image, i.e., $\vec{b}$ has the same sign for each dislocation.

The dislocations in the network do not all lie at exactly the same depth. For example in Fig. 4 part of the network has been polished away while other segments still remain within the foil. This is also shown by the tendency for two or more lines to attract each other. This would only be so for edge dislocations of the same sign if they lie at different depths. In Fig. 2 there are many examples of pairs or larger clusters. In Fig. 5 six dislocations lying approximately one above the other were observed. The fact that the vertical allignment was usually not perfect suggests that even at the diffusion temperature the glide mobility of these dislocations was not great. This might be expected because they do not lie in their {111} glide planes: they must glide in (001) in order to line up one above another.

The numbers of dislocations in the array is difficult to measure accurately because so many of the lines correspond to more than one dislocation. However, there are roughly ten dislocations per micron. This would correspond to a change in the lattice parameter of about 0.4%. The ionic radii of silicon and phosphorus are 1.17Å and 1.07Å respectively. Therefore, the array would accommodate the misfit due to a phosphorus concentration in the surface layers of the order of 4 atomic percent.

* All rotations between diffraction patterns and images have been taken into account in the Figures shown.

An interesting question concerning this type of array is the mechanism by which it moves into the crystal as the diffusion proceeds. Substitution of phosphorus atoms in silicon causes a decrease in lattice parameter. Therefore, if the dislocations shown in Fig. 2 climb into the crystal, there must be continuous migration of vacant lattice sites from the dislocations to the external surface. The electron micrographs show that climb does occur during the diffusion reaction. Helical dislocation segments were observed as shown in Fig. 6 (see also Fig. 4). In some areas there was also evidence for precipitation of solute elements, or vacancies or both together. Large numbers of small defects can be seen in regions away from the dislocations in Figs. 3, 4 and 6. At high magnifications these defects show diffraction contrast similar to that of dislocation loops or planar clusters of solute atoms that are accompanied by lattice strain. The image is smaller for $\vec{g}\cdot\vec{b}s < 0$ than for $\vec{g}\cdot\vec{b}s > 0$[4] and the visibility of the defects is orientation sensitive. At the present time, from contrast experiments alone it has not been possible to decide whether these defects are small dislocation loops or coherent solute atom clusters, or precipitates. However, the fact that the dislocation lines themselves were often decorated by strings of precipitates suggests that solute atoms were present in the defects. In Fig. 7 rows of precipitates can be seen where dislocations are out of contrast. It seems reasonable to assume that these precipitates contain phosphorus. In agreement with this hypothesis it has been found from an analysis of diffusion profiles[8] that for heavy concentrations only a fraction of the phosphorus is active as a donor. The rest might be assumed to be precipitated.

Not all of the dislocations in the array had Burgers vectors a/2[110] or a/2[$\bar{1}$10]. The presence of some lines with Burgers vectors that were not

parallel to the surface of the specimen suggested another mechanism by which the network could be formed. The long edge dislocations that comprised the majority of the network always terminated at nodes. The contrast experiment illustrated in Fig. 8 shows three vertical dislocation lines that do not go out of contrast when only diffraction plane (3) is operating (Fig. 8b). Therefore, unlike the majority of the dislocations that lie along direction BC they do not have Burgers vector AD. It can also be seen that many of the edge dislocations lying along AD terminate at nodes along these three singular lines. Furthermore, the dislocations that end at the lines come alternately from one side and then the other. Another feature that is illustrated clearly by Fig. 9 is that all the individual segments of a given singular line are often bowed in the same direction which suggests that the line was in motion. This would result in shortening the edge dislocations terminating at the line from one side and lengthening of those that approach it from the other side. Singular lines sometimes turn from the general direction AD into the general direction BC so that both those edge dislocations lying along AD and those parallel to BC can terminate at different parts of the same singular line. Examples of this can be seen both in Fig. 8 and 9.

These observations suggest that the mechanism by which the crossed grid of edge dislocations is removed from a given depth and reformed at a greater depth is by glide of singular lines that have Burgers vectors AB, DB, CD or CA. By this mechanism the network can follow the diffusion primarily by glide motions rather than entirely by climb. Growth of a network at one level at the expense of that at another level by motion of singular lines is illustrated schematically by Fig. 10. The Burgers vectors of all lines are labeled. Individual segments of singular lines can lie approximately on their glide planes.

The fact that only alternate segments of a singular line should have the same Burgers vector can also be confirmed by diffraction contrast. Figure 11 shows that for diffracting plane (1), alternate segments of the singular line marked "A" go out of contrast together. For diffracting planes (3), (220, or (4), $\bar{2}20$, singular lines were always entirely in good contrast as expected. The same area shown in Fig. 11 can be seen in Fig. 3 with all segments of line "A" in good contrast.

The mechanism governing formation and motion of the dislocations is apparently the following. Upon exposure to the P_2O_5, a very highly doped, shallow surface layer is formed. It is known[8] that the distribution coefficient for phosphorus between Si and SiO_2 is such that dissolution in Si is greatly favored. Thus one probably has a shallow layer of silicon, doped to the solid solubility limit, which is adjacent to the glass. In the specimens observed by transmission electron microscopy the glass layer had either been removed during preparation of the foil or it was extremely thin. It could not be detected either by optical or electron microscopy observations.

According to the rapidity of phosphorus diffusion and oxidation, the dislocations glide inside to follow the traveling zone of misfit. Glide is easiest for the 60° dislocations in (111) planes. When suitably oriented glide dislocations meet; a stable network is produced.*

It is interesting to consider also the case of doping with boron trioxide B_2O_3. Boron is also a substitutional impurity smaller than silicon. It has been shown to effectively create "diffusion-induced" dislocations and slip-patterns.[2, 3] Some faint contrast was observed in electron

---

* Similar but not as detailed conclusions can be drawn from x-ray topographs; Schwuttke and Queisser, unpublished.

microscope specimens. Figure 12 is an example; here the faint traces may correspond to etching grooves at dislocation sites or at previous positions of dislocations due to precipitates. Glassy layers containing B_2O_3, apparently do not cause networks of misfit dislocations near enough to the surface to be easily revealed by the thin foil technique. This result seems surprising, but may be explained by the distribution coefficient of B between Si and SiO_2. It is not yet clearly established, but seems plausible, that boron favors dissolution in the glassy SiO_2 layer rather than in the Si. This could cause the lack of a sharp impurity gradient within the silicon near the surface. When the network of misfit dislocations is farther from the surface than the thickness of an electron transparent foil then it is very difficult to prepare a foil that contains the network. Just the right amount of material must be removed by chemical polsihing from both sides of the original specimen. We have not yet been successful in preparing an electron microscope specimen containing misfit dislocations for boron diffused silicon.

Acknowledgements

The authors are pleased to acknowledge the financial support of the U.S. Atomic Energy Commission through the Inorganic Materials Research Division of the Lawrence Radiation Laboratory (J. W. and G. T.) and of the U.S. Army Research Office (H. J. Q.).

References

1. H. J. Queisser, J. Appl. Phys., 32, 1776 (1961).
2. S. Prussin, J. Appl. Phys., 32, 1876 (1961).
3. G. H. Schwuttke and H. J. Queisser, J. Appl. Phys., 33, 1540 (1962).
4. R. H. Finch, H. J. Queisser, G. Thomas and J. Washburn, J. Appl. Phys., 34, 406 (1963).
5. G. V. Patser and P. R. Swann, J. Sci. Instr., 39, 58 (1962).
6. P. B. Hirsch, A. Howie and M. J. Whelan, Phil. Trans. Roy. Soc., A 252, 499 (1962).
7. A. Howie and M. J. Whelan, Proc. Roy. Soc., A 267, 206 (1962).
8. M. M. Atalla and E. Tannenbaum, Bell Syst. Tech. Journ., 39, 933 (1960).

Figure Captions

Fig. 1. Tetrahedron of {111} planes as projected onto (001).

Fig. 2. Crossed grid of misfit dislocations due to diffusion of phosphorus into silicon, (a) Low magnification photograph showing a variety of different diffraction conditions. (b),(c),(d) Three different single diffraction images for the same area showing that the array is a crossed grid of edge dislocations with Burgers vectors parallel to the (001) surface. (see text).

Fig. 3. Double images due to the operation of the two reflections 400 and 220 showing that all dislocations in a given set have the same sign. Notice also the large number of loop-like defects. (see text).

Fig. 4. Area in which part of the network has been polished away showing that all of the lines are not at exactly the same depth. Notice helical dislocation at A.

Fig. 5. A cluster of several dislocation of the same sign showing tendency for lines at different depths to line up one above the other.

Fig. 6. Evidence for dislocation climb - note helical dislocation segment and small loop-like contrast.

Fig. 7. Evidence for precipitation along dislocation lines. Note strings of precipitate that are visible where some dislocations are out of diffraction contrast.

Fig. 8. (a),(b), Diffraction contrast experiment showing that some singular lines are present that do not have Burgers vectors that are parallel to the surface of the specimen. In (a) the 040 and $\bar{2}\bar{2}0$ reflections operate, in (b) only the 220 reflection operates (see text for explanation).

Fig. 9. Network lines terminating at singular lines that are bowed suggesting that they were in motion.

Fig. 10. Suggested mechanism for the transfer of a network from one level to another by the motion of singular lines.

Fig. 11. Same area as Fig. 3 but for single 400 diffraction condition showing that singular lines consist of segments having different Burgers vectors. In this case alternate segments having the same Burgers vector are out of good contrast.

Fig. 12. Faint traces along [$\bar{1}$10] and [110] directions in silicon after a B_2O_3 doping treatment orientation [001].

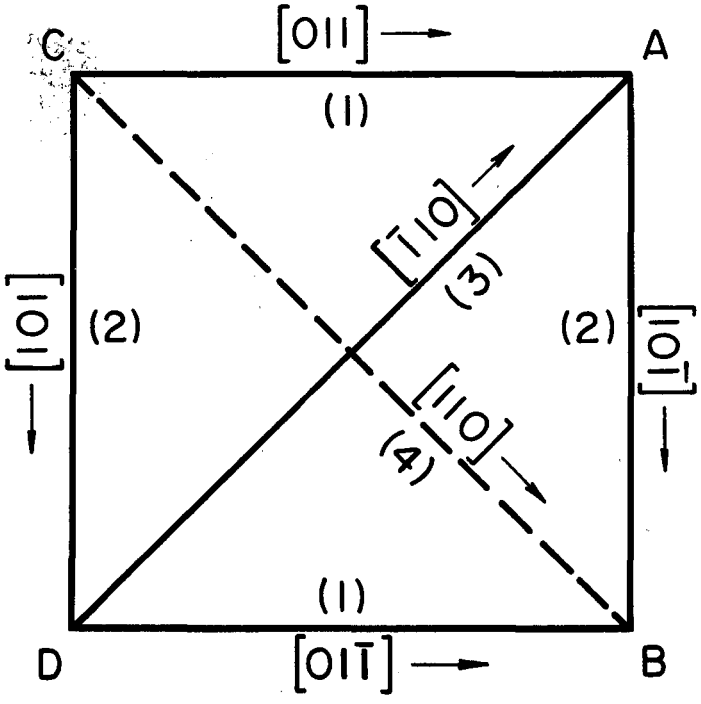

ADB = (111)
ADC = ($\bar{1}\bar{1}$1)
ACB = (1$\bar{1}$1)
DCB = ($\bar{1}$11)

MU-32775

Fig. 1

Fig. 2(a)

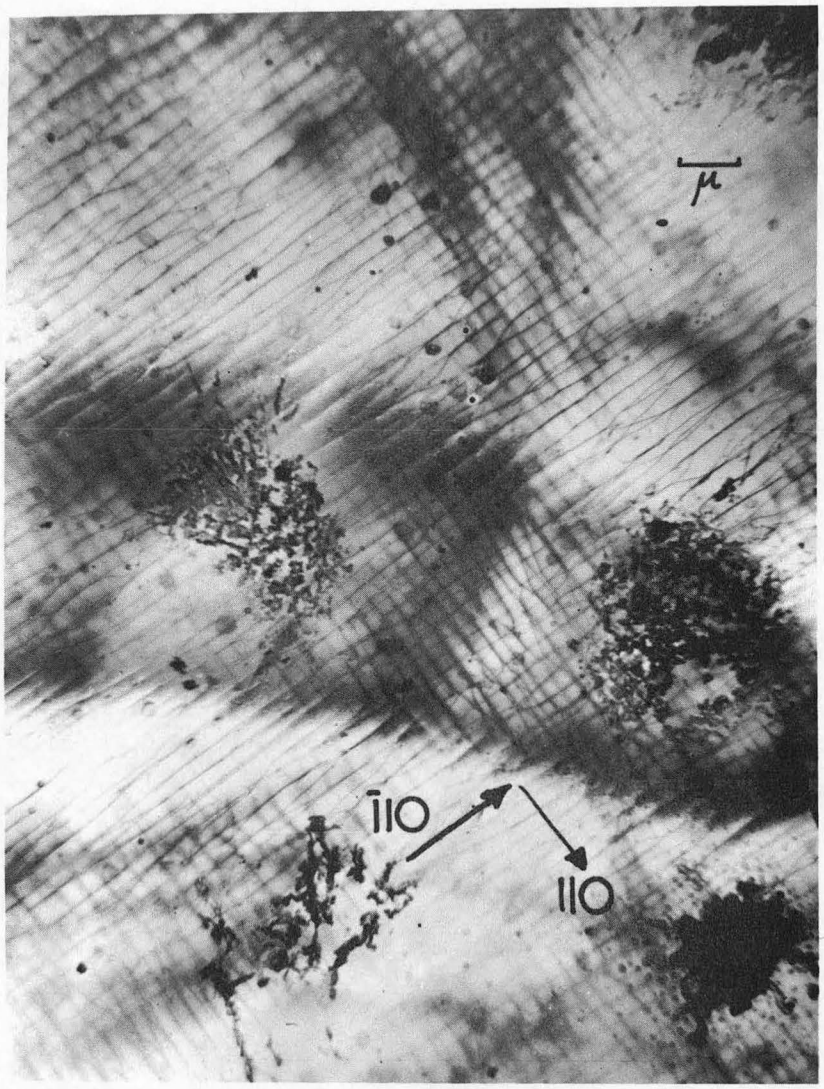

ZN-4122

Fig. 2(a)

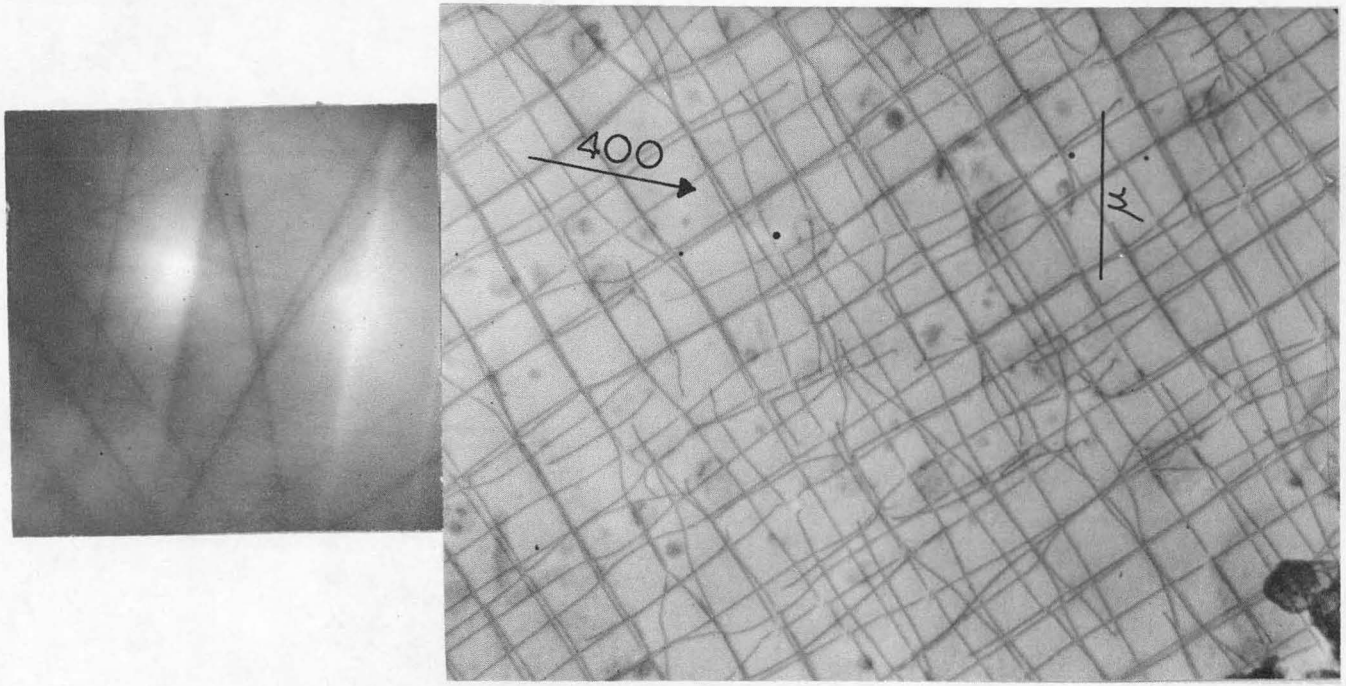

ZN-4142

Fig. 2(b)

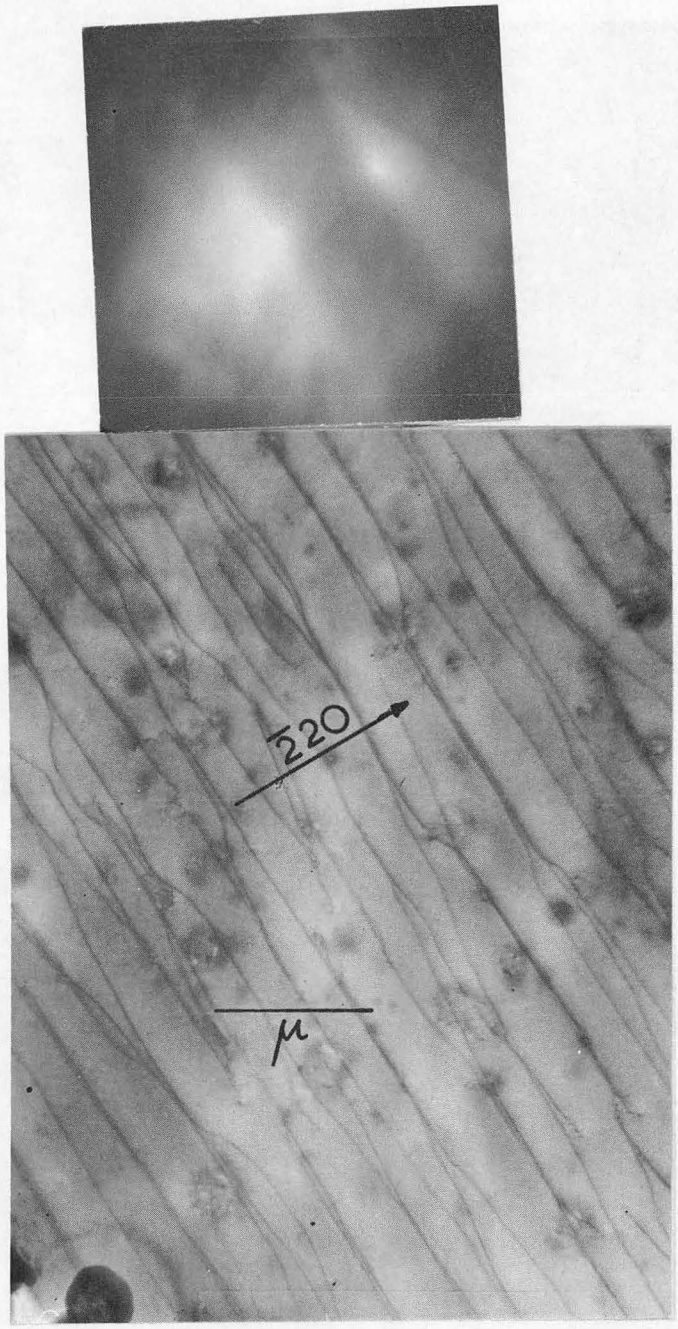

Fig. 2(c)

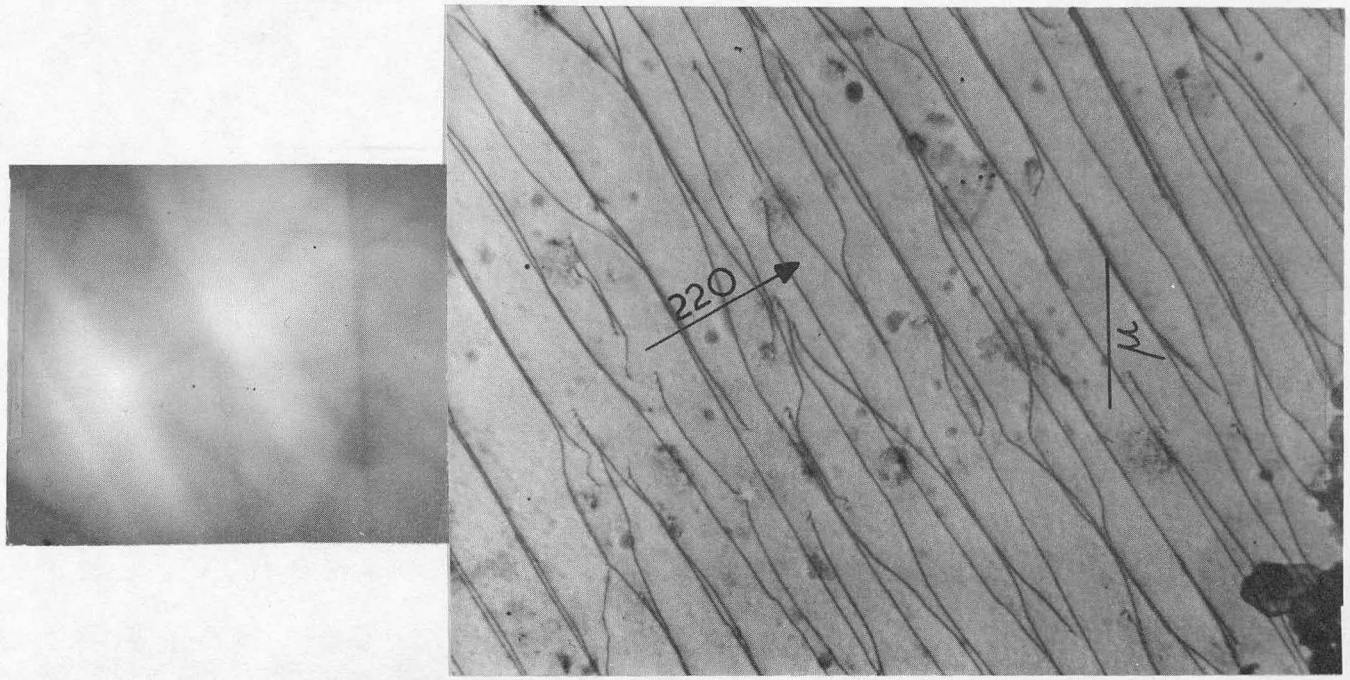

ZN-4144

Fig. 2(d)

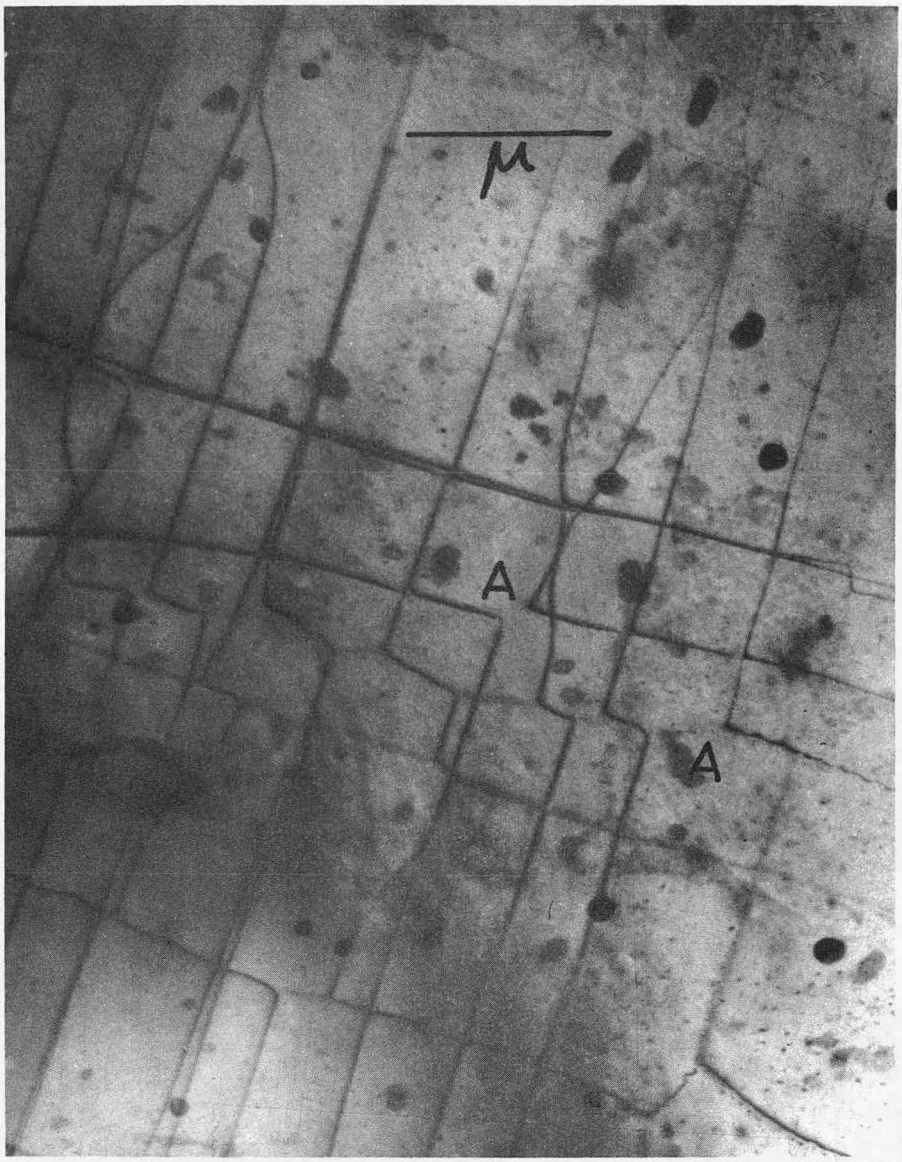

ZN-4123

Fig. 3

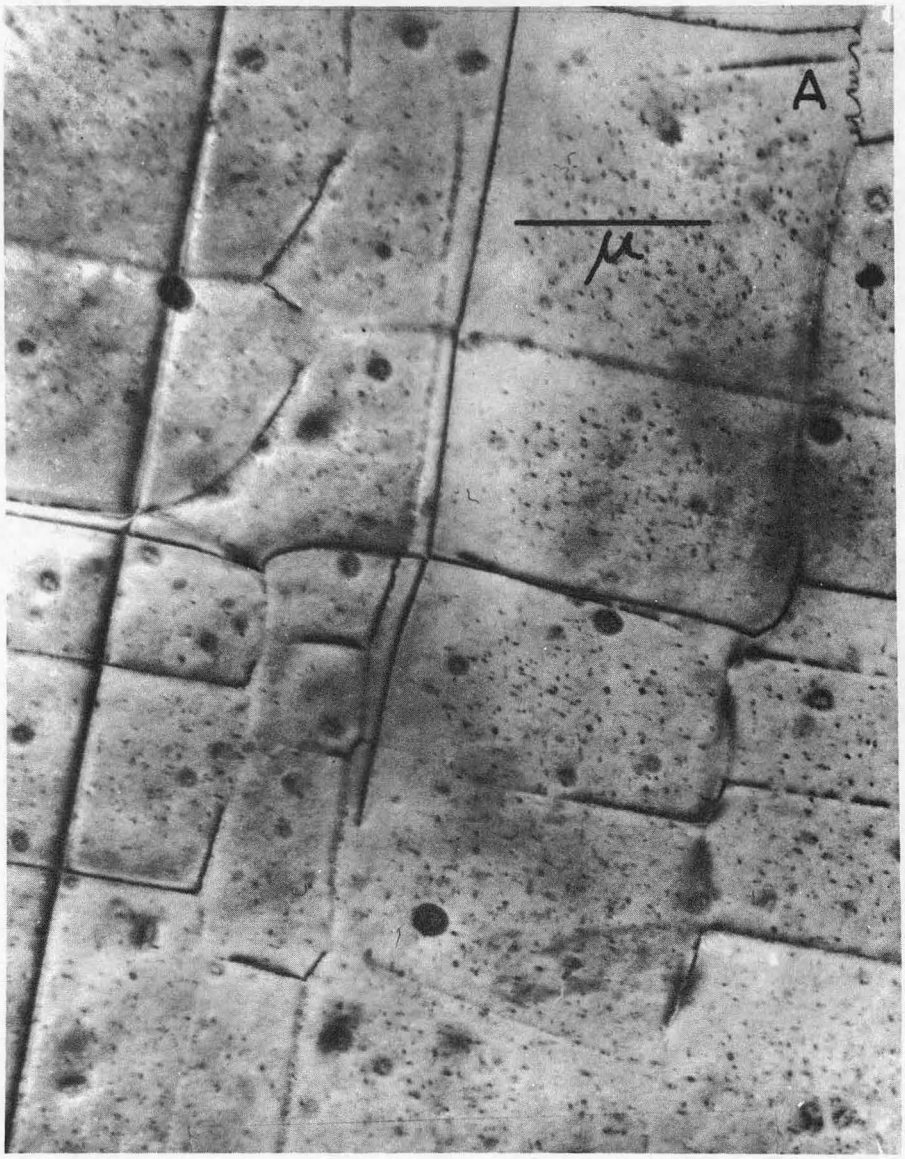

ZN-4124

Fig. 4

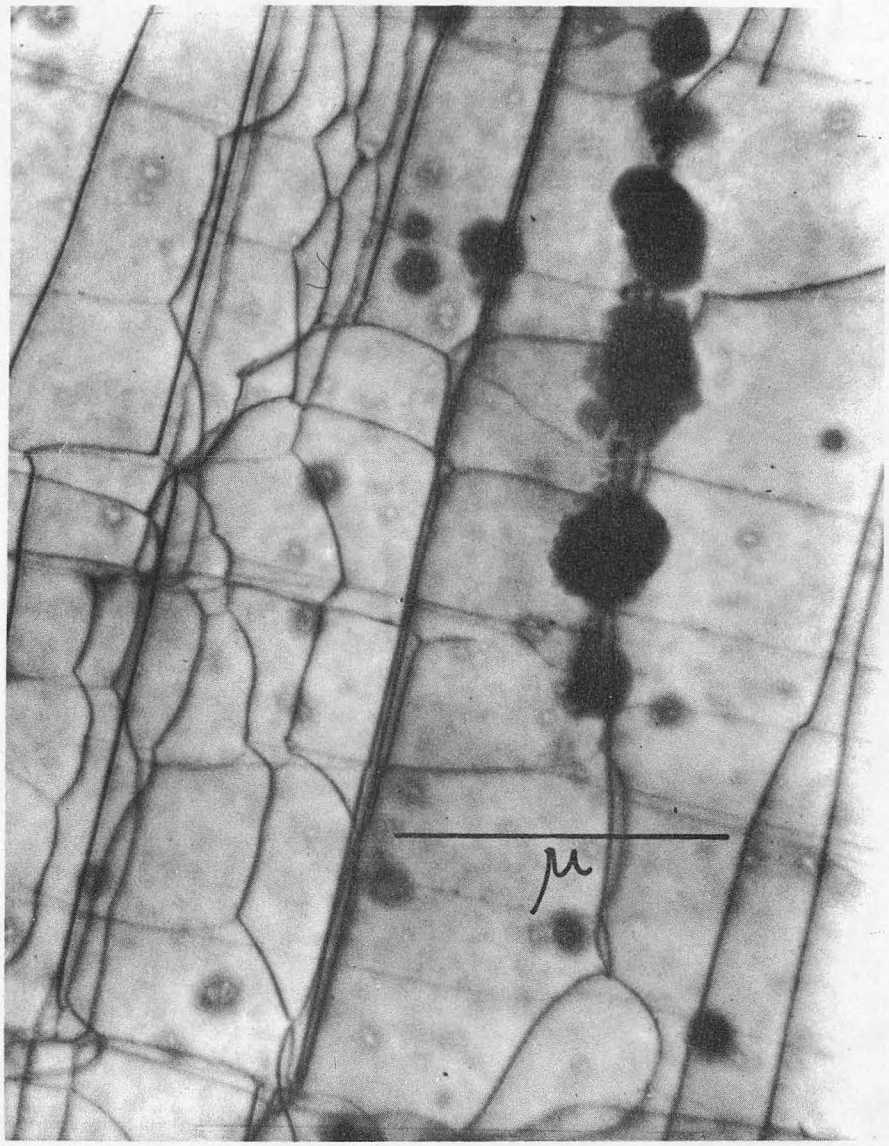

ZN-4125

Fig. 5

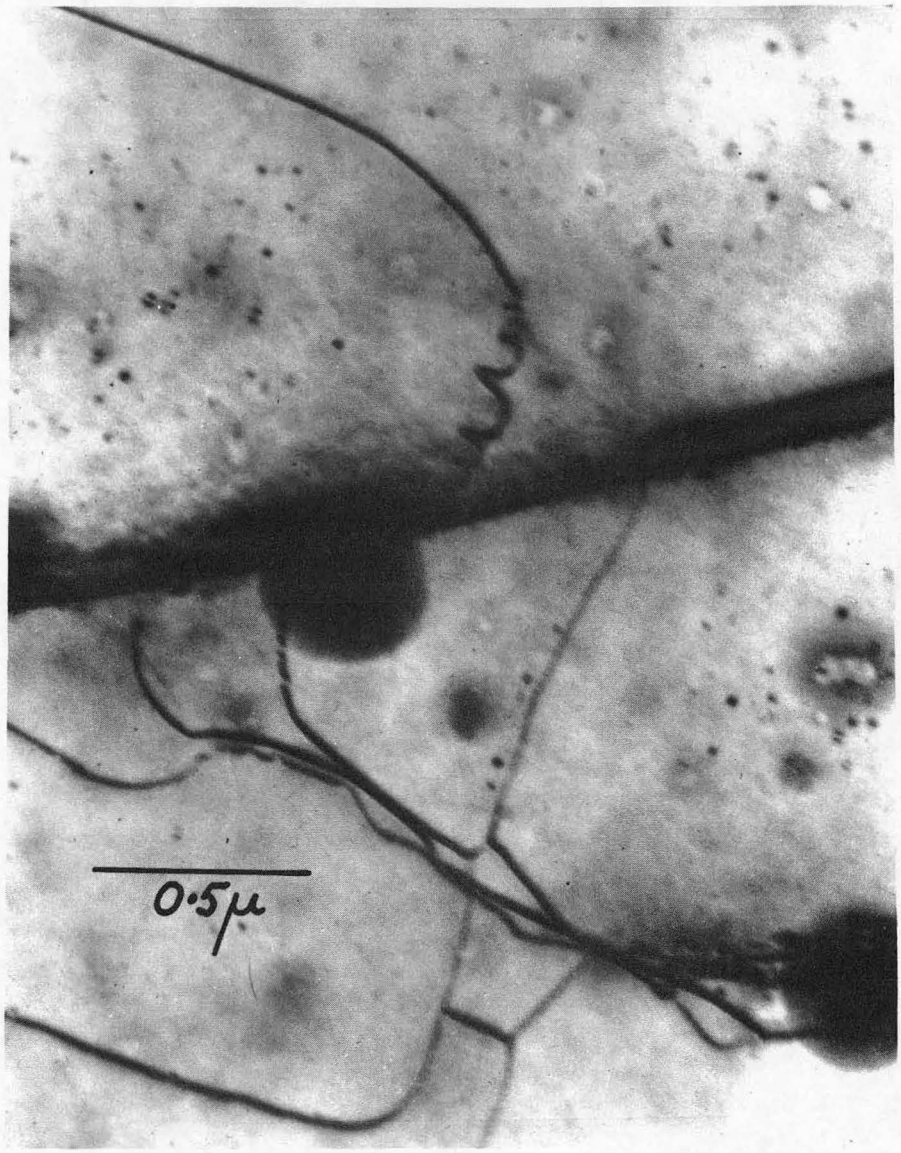

ZN-4126

Fig. 6

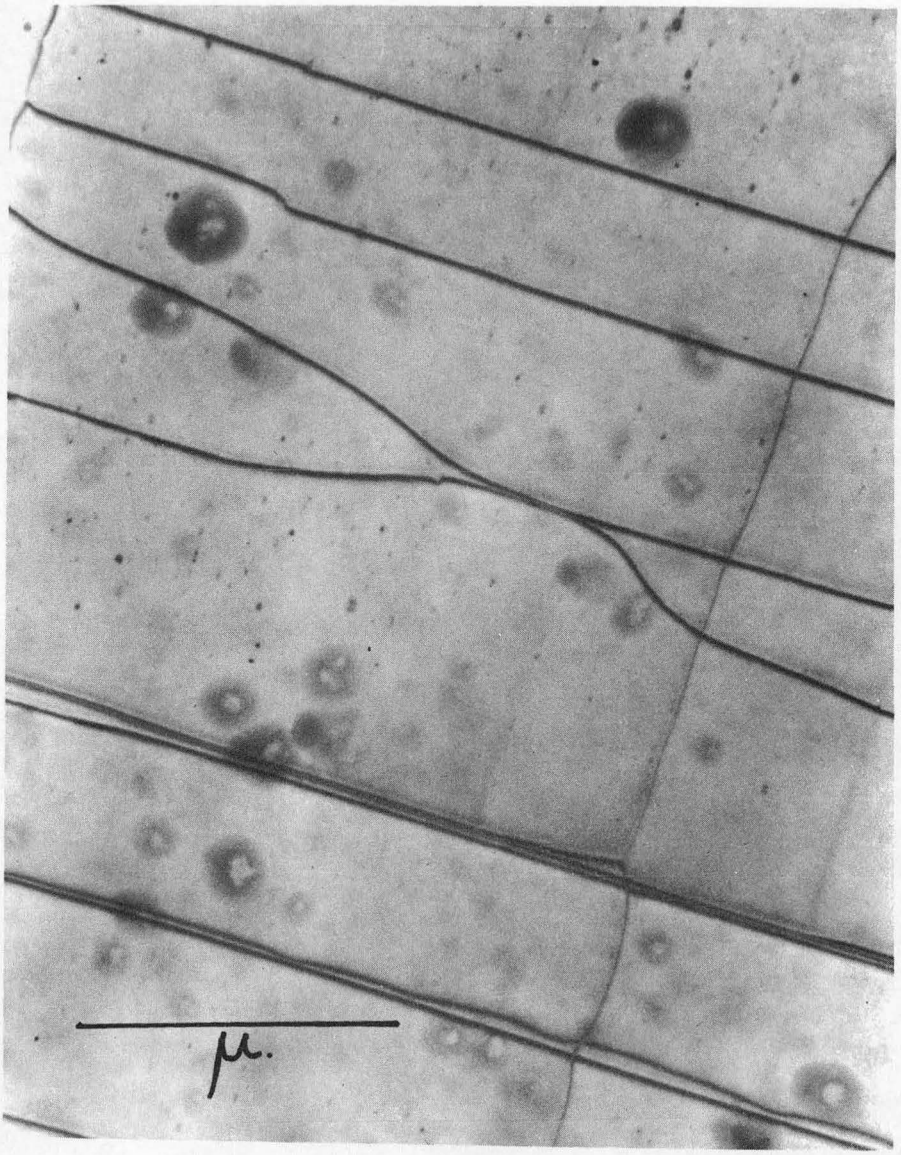

ZN-4127

Fig. 7

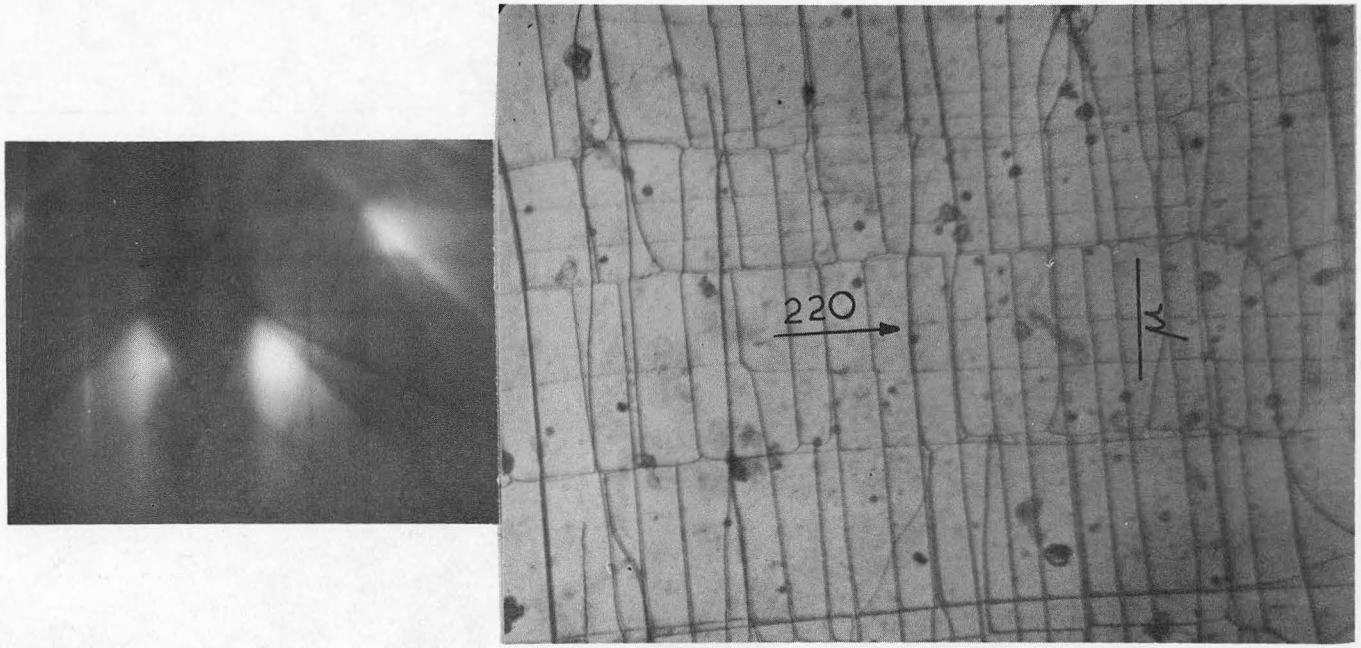

ZN-4145

Fig. 8(a)

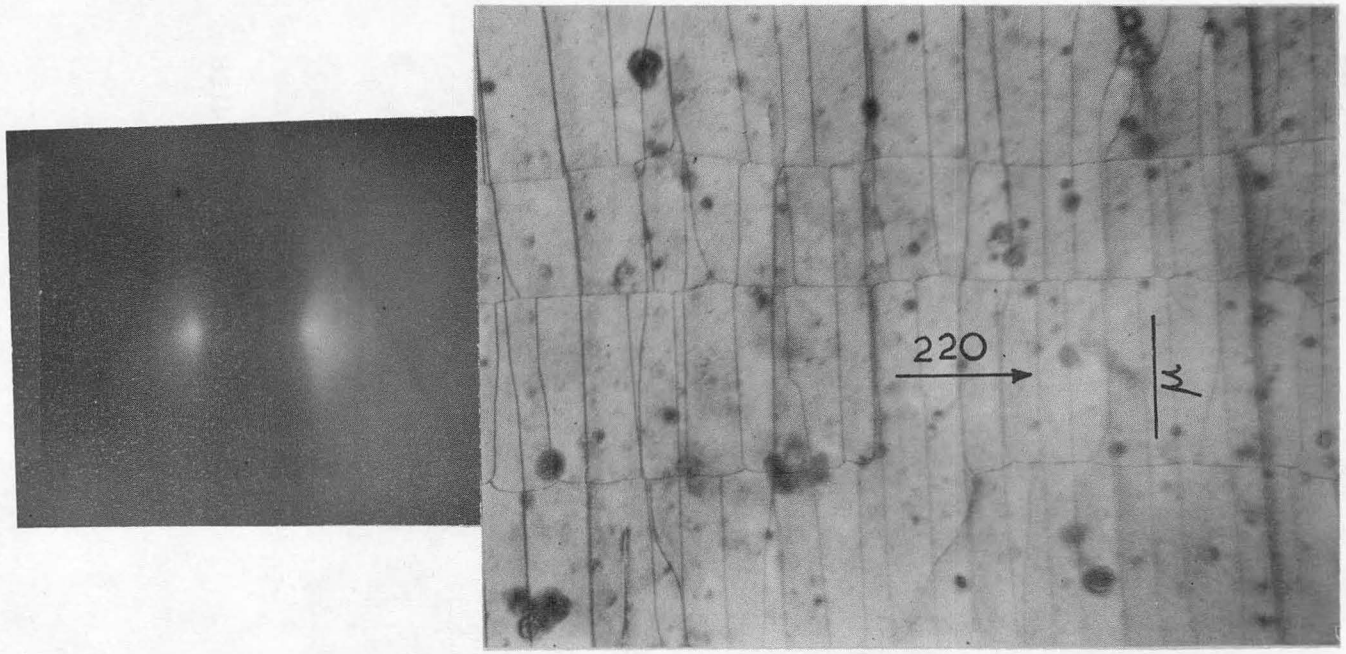

ZN-4146

Fig. 8(b)

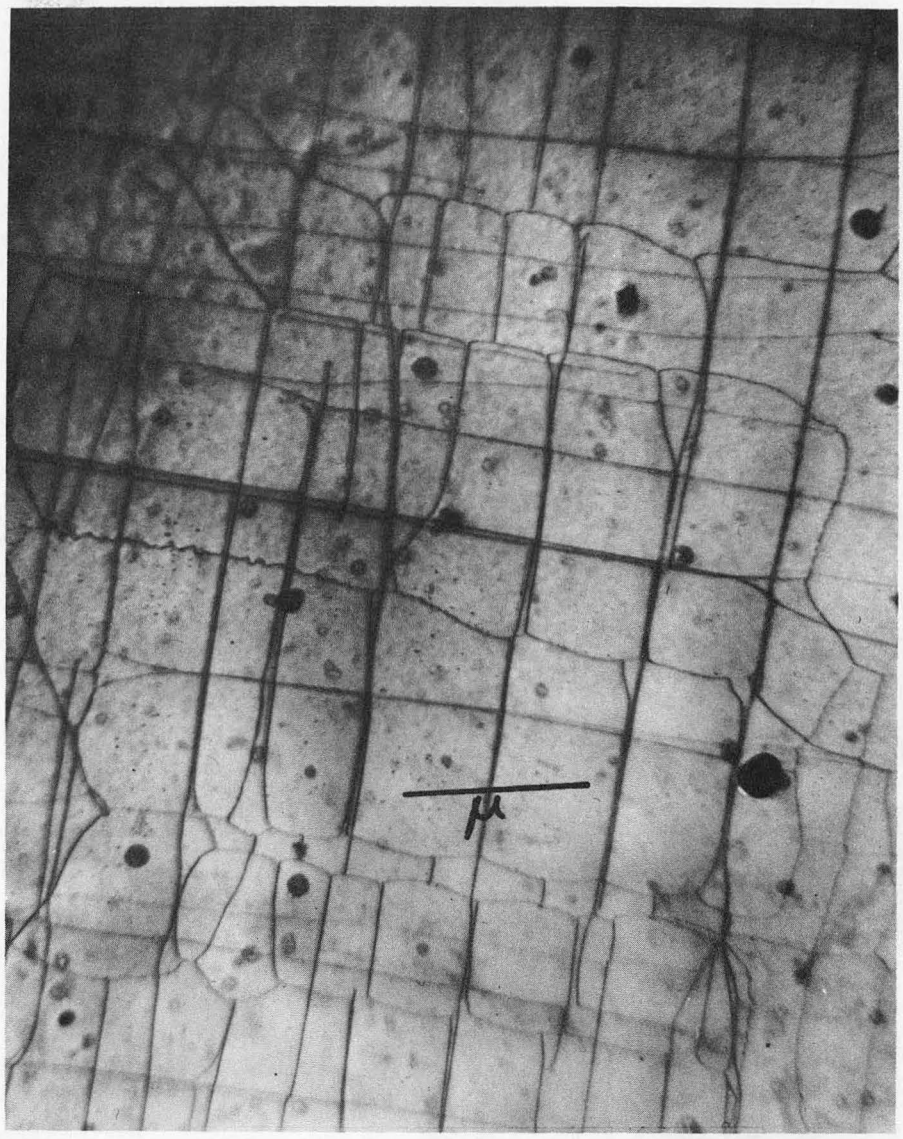

ZN-4128

Fig. 9

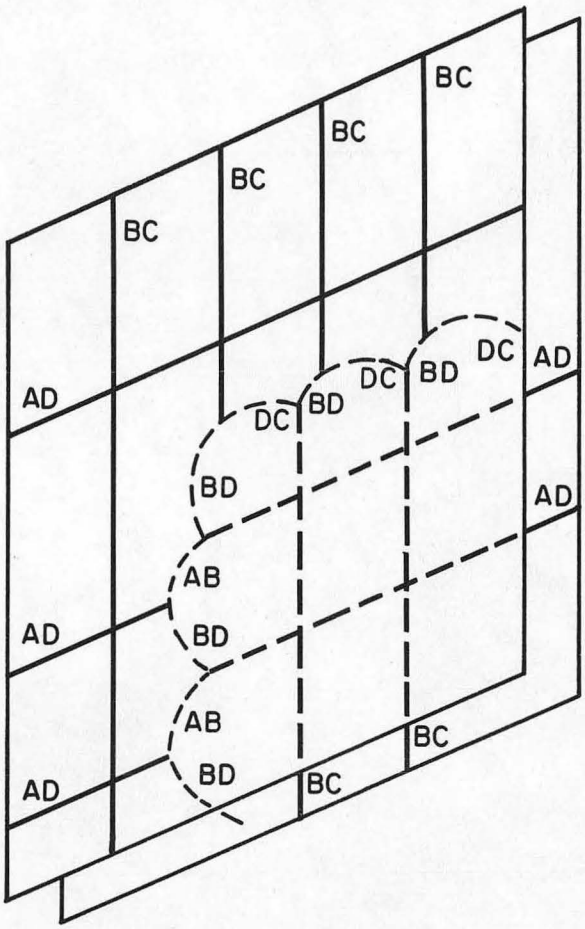

MU-32776

Fig. 10

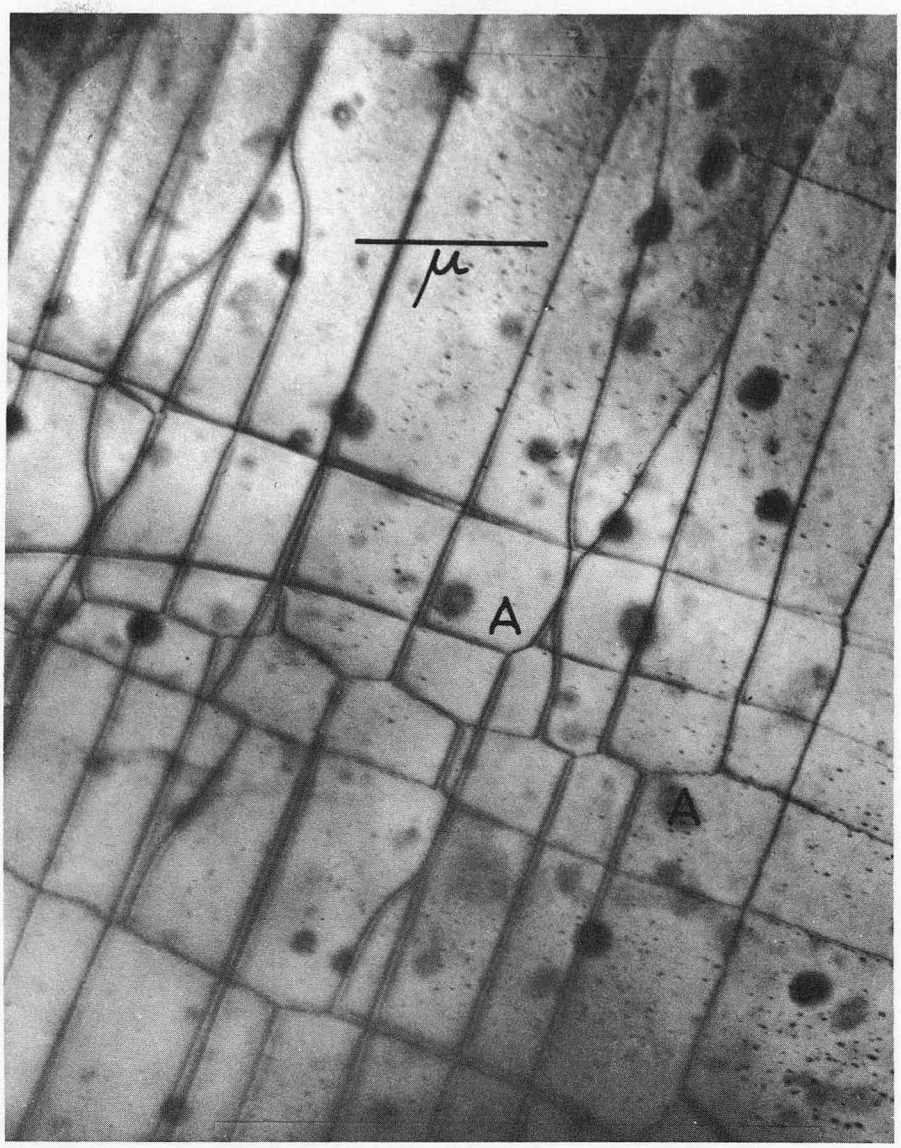

ZN-4129

Fig. 11

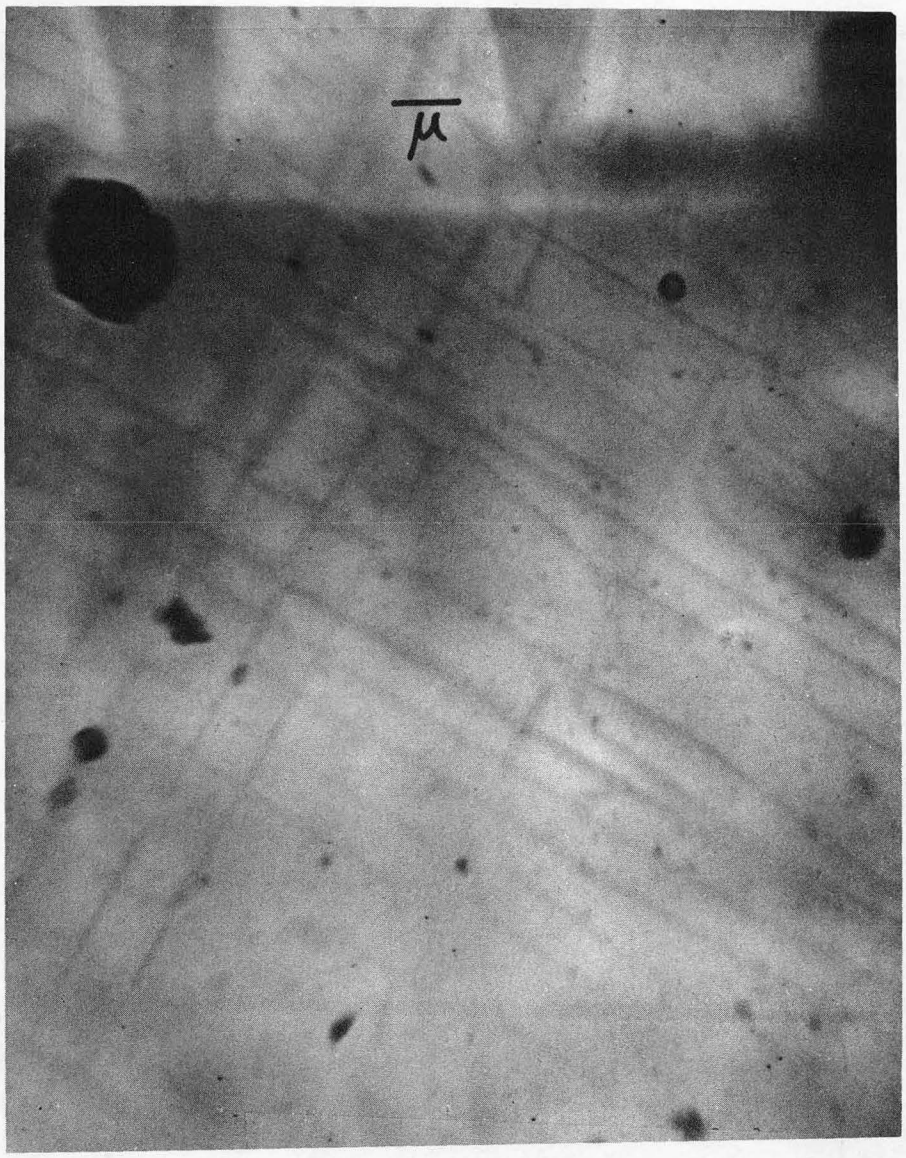

ZN-4130

Fig. 12

This report was prepared as an account of Government sponsored work. Neither the United States, nor the Commission, nor any person acting on behalf of the Commission:

A. Makes any warranty or representation, expressed or implied, with respect to the accuracy, completeness, or usefulness of the information contained in this report, or that the use of any information, apparatus, method, or process disclosed in this report may not infringe privately owned rights; or

B. Assumes any liabilities with respect to the use of, or for damages resulting from the use of any information, apparatus, method, or process disclosed in this report.

As used in the above, "person acting on behalf of the Commission" includes any employee or contractor of the Commission, or employee of such contractor, to the extent that such employee or contractor of the Commission, or employee of such contractor prepares, disseminates, or provides access to, any information pursuant to his employment or contract with the Commission, or his employment with such contractor.